

## Iron ore classification by XRD-Rietveld and cluster analysis

### *Classificação de minério de ferro por DRX-Rietveld e análise de agrupamento*

Fábio Ramos Dias de Andrade<sup>1</sup>, Luciano de Andrade Gobbo<sup>2</sup>, Lyvia Fernanda Amaral Sousa<sup>1</sup>

<sup>1</sup>Instituto de Geociências, Departamento de Mineralogia e Geotectônica, Universidade de São Paulo - USP, Rua do Lago, 562, CEP 05586-010, São Paulo, SP, BR (dias@usp.br; lyvia.sousa@gmail.com)

<sup>2</sup>PANalytical Inc., São Paulo, SP, BR (luciano.gobbo@panalytical.com)

Received on June 2<sup>nd</sup>, 2015; accepted on February 15<sup>th</sup>, 2016

#### **Abstract**

This study establishes a routine for quantitative phase analysis by X-ray diffraction (XRD-Rietveld) in iron ore samples. Studied samples came from Quadrilátero Ferrífero, Southeastern Brazil, and are mainly composed by hematite, magnetite, goethite, quartz and kaolinite, being divided in three clusters: cluster 1 ( $n = 8$ ), characterized by the presence of hydrated phases goethite (25 to 72 wt %), kaolinite (< 25 wt %) and gibbsite (< 10 wt %), plus hematite (7 to 54 wt %) and quartz (2 to 19 wt %); cluster 2 ( $n = 16$ ), which consists of hematite (22 to 81 wt %) and quartz (2 to 58 wt %) and smaller proportions of goethite (< 22 wt %) and kaolinite (< 13 wt %); and cluster 3 ( $n = 3$ ), that has a predominance of quartz (62 to 74 wt %) and smaller amounts of hematite (17 to 33 wt %) and kaolinite (< 5 wt %). Classification of ores by XRD-Rietveld and cluster analysis is a fast, low-cost and reliable option for substituting ore classification with chemical analysis.

**Keywords:** Iron ore; X-ray diffraction; Rietveld method; Cluster analysis.

#### **Resumo**

Este trabalho estabelece uma rotina de análise quantitativa de fases por difração de raios X (DRX-Rietveld) em minério de ferro. As amostras analisadas são provenientes do Quadrilátero Ferrífero, Sudeste do Brasil, sendo compostas por hematita, magnetita, goethita, quartzo e caulinita, tendo sido classificadas em três agrupamentos: agrupamento 1 ( $n = 8$ ), caracterizado pela presença das fases de alteração goethita (25 a 72% em peso), caulinita (< 25% em peso) e gibbsita (< 10% em peso), além de hematita (7 a 54% em peso) e quartzo (2 a 19% em peso); agrupamento 2 ( $n = 16$ ), com amostras compostas por hematita (22 a 81% em peso) e quartzo (2 a 58% em peso), com proporções menores de goethita (< 22% em peso) e caulinita (< 13% em peso); agrupamento 3 ( $n = 3$ ), contendo amostras com predomínio de quartzo (62 a 74% em peso) e proporções menores de hematita (17 a 33% em peso) e caulinita (< 5% em peso). A classificação de minérios de ferro por DRX-Rietveld e análise de agrupamento é uma opção rápida, confiável e de baixo custo para substituir a classificação de minérios por análises químicas.

**Palavras-chaves:** Minério de ferro; Difração de raios X; Método de Rietveld; Análise de agrupamento.

## INTRODUCTION

Brazil is the third largest iron ore producer, following China and Australia. Iron is the main mineral commodity in Brazil and corresponded to 78% of exports in the mineral sector in the first semester of 2014 (DNPM, 2013; 2014). Classification of iron ores in mining plants is typically based on chemical data. Although largely used, chemical criteria do not provide information on the mineralogical composition, particularly on the relative proportion of the mineral phases of the ore. The iron content of the ore depends on the relative proportion of iron-bearing minerals magnetite ( $\text{Fe}_3\text{O}_4$ , 72.4 wt % Fe), hematite ( $\text{Fe}_2\text{O}_3$ , 69.9 wt % Fe) and goethite ( $\text{FeO}(\text{OH})$ , 59.9 wt % Fe). Goethite has the highest amount of impurities and water, and water release during sintering increases porosity in the sinter (Pena et al., 2003).

Mineral composition of iron ores directly impacts  $\text{CO}_2$  emission and energy consumption in iron production, as the  $\text{Fe}^{2+}/\text{Fe}^{3+}$  ratio determines the amount of coke and energy needed to reduce the oxides to metal (Knorr and Young, 2011). Additionally, XRD is useful to identify mill scales in the ore, which will not be identified by chemical methods. The combined use of mineralogical and chemical data collected with different techniques has received increased attention, in a field known as geometallurgy (Parian et al., 2015).

Although the ore displays a rather continuum compositional range, clusters provide a simple way to classify samples according to their main mineralogical features. Combined XRD-Rietveld and cluster analyses may be developed from a relatively small group of samples, at the starting point of an automated procedure of ore classification in industrial plants. A practical advantage of cluster analyses is that a large number of samples may be ascribed to discrete categories or clusters, based on their raw XRD patterns. Individual interpretation of XRD data is not necessary, as long as mineralogical compositions of representative samples of each cluster are well defined and the whole diversity of a given deposit or blend is considered. Once this framework is available, ordinary samples can be classified in one of the available clusters on a routine basis. The number of clusters is arbitrarily defined by the operator and may be reviewed at any time. If the ore composition changes significantly and the samples cannot be classified in the available clusters, those samples will be called non-clustered samples.

As the XRD-Rietveld method of quantitative phase analysis is based on mathematical models, its results have to be cross-checked for consistency, which is usually made with chemical data. Once this consistency is achieved for a particular system, such as a hematite-magnetite-goethite-quartz ore, similar samples may be analysed with the same strategy, providing reliable results. Recent examples of XRD-Rietveld application in mining and metallurgy include studies by Antoniassi et al. (2008) and Shimizu et al. (2012).

This study presents a classification of iron ores based on mineralogical analysis, using the X-ray diffraction (XRD) Rietveld method of quantitative phase analysis and cluster analysis as a low cost alternative to chemical classification of ores. Studied samples are extracted from hematitic ores from Quadrilátero Ferrífero Mineral Province, Southeastern Brazil. Quantitative phase analysis was cross-checked with chemical data.

## SAMPLES AND ANALYTICAL METHODS

This study was carried out on 27 samples of hematitic iron ore from Central Quarry of Itatiaiuçu, Quadrilátero Ferrífero, also known as Iron Quadrangle, Southeastern Brazil. Samples were provided by Usiminas S.A.

Quadrilátero Ferrífero is a major Archean mineral province, initially defined by Dorr (1969) and subsequently studied by several authors (e. g., Babinski et al., 1993; Chemale Júnior et al., 1994; Renger et al., 1995; Rosière and Chemale Júnior, 2001).

Samples were taken as such, quartered and hand-grinded in chalcedony mortar. XRD was collected in a PANalytical CubiX<sup>3</sup> diffractometer at Usiminas S.A. mineralogy laboratory, with cobalt Ka radiation ( $\lambda = 1.790 \text{ \AA}$ ), 45 kV, 40 mA, spinning sample holder, angular interval from 10 to 80° 2 $\theta$ , step size 0.01° 2 $\theta$ , 5 seconds/step, automatic divergent slit receiving slit 0.1 mm. Cobalt radiation was used to avoid background enhancement due to secondary fluorescence, which occurs in iron-rich materials analysed under copper Ka radiation.

The Rietveld method (Rietveld, 1969) is based on the mathematical simulation of a diffractogram. The calculated diffractogram is refined in iteration steps in order to converge towards the observed diffractogram of the sample. Calculated diffractograms are based on the crystallographic parameters of the mineral phases present in the sample and on the instrumental parameters used in data collection. In this study, the Rietveld analysis was performed using the PANalytical High Score Plus 3.0. The overall refinement strategy started with automatic background detection, insertion of structure of phases, correction of specimen displacement, refinement of cell parameters for each phase, full-width at half-maximum (FWHM) with the W term of the function described by Caglioti et al. (1958), peak asymmetry and preferred orientation of hematite and kaolinite (001). Details on Rietveld guidelines are discussed by McCusker et al. (1999). The phases identified and respective references of crystallographic information files are the following: quartz (Ikuta et al., 2007), hematite (Sawada, 1996), magnetite (Levy et al., 2012), goethite with Al substitution (Li and O'Connor, 2006), kaolinite (Bish and von Dreele, 1989) and gibbsite (Saalfeld and Wedde, 1974), all available at the Crystallographic Open Database (COD) (Grazulis et al., 2009).

The cluster analysis of the collected diffractograms was also performed using Panalytical High Score Plus 3.0. Diffractograms were gathered in three clusters, considering: (i) profiles as data source; (ii) comparison of position + intensity of peaks; (iii) intensity threshold = 0.75; (iv) pattern shifts allowed up to  $0.5^\circ 2\theta$ ; (v) Euclidian distance measurement; (vi) average linkage method; (vii) manual cut-off method, actual cut-off value 115 (range 15-1000). Cluster analysis is a practical method to compare large data sets based on their numerical similarity. For details on the theory, see Everitt and Landau (2011).

Iron ore samples and respective chemical data were provided by Usiminas S.A. Chemical composition was determined by X-ray fluorescence (XRF) in pressed pellets in a PANalytical AXIOS spectrometer.

Results of quantitative phase analysis by XRD-Rietveld were cross-checked with the XRF-determined chemical composition of each sample. As XRF is a method with high reproducibility and narrow standard deviation, it is used here as an external reference to check the quality of XRD-Rietveld refinement results. Weight fractions of the minerals in each sample were combined with the atomic proportion (wt %) of Fe and Si in the ideal chemical composition of the minerals, using stoichiometric conversion factors. Total iron content ( $Fe_{total}$ ) was calculated as it follows:

$$Fe_{total} = 0.699 X_{hm} + 0.724 X_{mt} + 0.599 X_{go} \quad (1)$$

where  $X_{hm}$ ,  $X_{mt}$  and  $X_{go}$  correspond to the weight fractions of hematite, magnetite and goethite (with Al substitution), respectively, in the studied samples.

Total silicon content ( $Si_{total}$ ) was calculated in a similar way:

$$Si_{total} = 0.467 X_{qz} + 0.217 X_{ka} \quad (2)$$

where  $X_{qz}$  and  $X_{ka}$  correspond to the weight fractions of quartz and kaolinite, respectively.

## RESULTS AND DISCUSSION

The iron ore samples analysed in this study are mainly composed by hematite, magnetite, goethite, quartz and kaolinite, with minor amounts of gibbsite. Diffraction peaks of these minerals show little overlapping (Figure 1), which favours XRD analysis. A Rietveld plot of sample 3, the most representative sample of the largest cluster (cluster 2), is presented in Figure 2. The residue line in the lower part of the plot shows mostly negative residues at  $2\theta$  angles lower than  $42^\circ$ , becoming positive and increasingly higher at higher angles; an increased background toward higher  $2\theta$  angles is also

observed. These features are a consequence of the automatic divergence slit used for data collection.

Chemical data provided by the mining company are presented in Table 1.  $Fe_2O_3$  contents vary from 40 to 96 wt %, with exception of sample 25 (24 wt %  $Fe_2O_3$ ).  $Al_2O_3$  ranges from 0.52 to 17.5 wt %, and the main Al-bearing mineral phase is kaolinite. Loss on ignition (LOI) ranges from 0.35 to 9.51 wt %, due to the presence of hydrated mineral phases (goethite, kaolinite and gibbsite).

Mineralogical composition determined by XRD-Rietveld is presented in Table 2, where samples are sorted according to their clusters. Three clusters were defined with distinct mineralogical compositions (Figure 3). Cluster 1 ( $n = 8$ ) is characterized by the presence of relatively large proportions of hydrated minerals goethite (25 to 72 wt %), kaolinite (up to 25 wt %) and gibbsite (up to 10 wt %), together with hematite (7 to 54 wt %) and quartz (2 to 19 wt %). Cluster 2 ( $n = 16$ ) is composed predominantly by hematite (22 to 81 wt %) and quartz (2 to 58 wt %), with smaller amounts

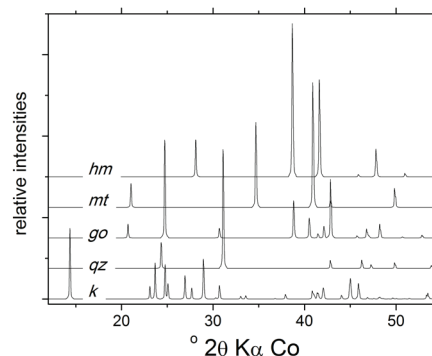
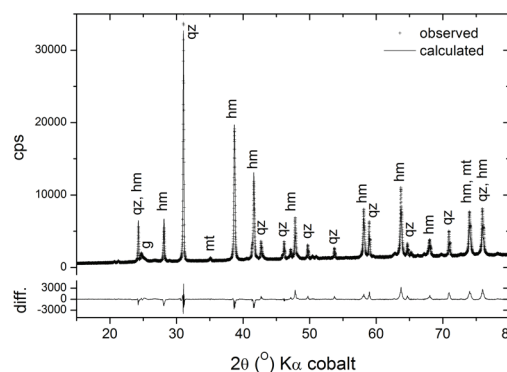


**Figure 1.** Calculated powder diffractograms of the ore minerals hematite (hm), magnetite (mt), goethite (go), quartz (qz) and kaolinite (k), using cobalt Ka radiation ( $\lambda = 1.790 \text{ \AA}$ ).



Hm: hematite; qz: quartz; mt: magnetite; g: goethite; CPS: counts per second; diff: difference.

**Figure 2.** Rietveld plot of iron ore sample no. 3, which is the representative sample of cluster 2.

of goethite (up to 22 wt %) and kaolinite (up to 13 wt %). Cluster 3 ( $n = 3$ ) is composed predominantly by quartz (62 to 74 wt %), with smaller amounts of hematite (17 to 33 wt %) and kaolinite (up to 5 wt %). Magnetite displays a non-regular distribution among the clusters, and its abundance is not related to total iron content or other chemical parameters. The three clusters may be clearly identified based on the relative proportions of quartz and goethite (Figure 4). Quality of Rietveld refinements is demonstrated by weighted residue of least square adjustment, which ranges from 10 to 18.2 (Table 2). For details on the meaning of statistical parameters of convergence, see Toby (2006).

Results of XRD-Rietveld analysis were cross-checked with whole rock chemical data (XRF). The elemental abundances of Fe and Si (wt %) were weighted according to the weight proportions of their respective phases, and plotted against the Fe and Si (wt %) abundances of the whole rock determined by XRF (Figure 5). Correlation coefficients for Fe ( $R^2 = 0.9034$ ) and Si ( $R^2 = 0.9406$ ) show a good consistency between XRD and XRF. Discrepancies are possibly related to the presence of poorly crystallized phases, particularly goethite, which causes a slight underestimation of Fe contents

**Table 1.** Chemical composition of the iron ore samples.

Sample	wt %						Total
	Fe <sub>2</sub> O <sub>3</sub>	SiO <sub>2</sub>	P <sub>2</sub> O <sub>5</sub>	MnO	Al <sub>2</sub> O <sub>3</sub>	LOI	
1	41.6	58.2	0.03	0.02	0.52	0.35	100.8
2	58.6	41.2	0.06	0.00	0.63	0.62	101.1
3	64.7	33.7	0.09	0.02	0.88	1.10	100.4
4	86.5	8.11	0.16	0.06	1.69	5.17	101.7
5	63.1	22.5	0.55	2.16	3.02	8.67	99.9
6	73.7	24.3	0.11	0.57	1.33	1.40	101.5
7	46.9	27.5	0.16	0.09	13.3	11.7	99.7
8	84.1	6.68	0.23	0.08	1.77	8.39	101.3
9	91.1	4.51	0.10	0.04	1.97	2.18	99.9
10	48.3	45.8	0.25	0.82	1.70	3.11	100.0
11	66.7	28.9	1.96	0.10	0.92	2.52	101.2
12	39.5	55.8	0.12	0.28	2.69	2.67	101.0
13	43.9	54.4	0.08	0.47	0.77	0.8	100.4
14	67.8	20.5	0.30	0.11	6.14	5.24	100.1
15	68.5	29.1	0.09	0.40	0.52	2.39	101.0
16	96.4	3.35	0.27	0.05	0.58	1.79	102.4
17	52.0	42.4	0.08	0.16	2.33	2.96	99.9
19	94.0	5.38	0.07	0.03	0.83	0.93	101.2
20	44.8	24.9	0.25	0.09	17.5	11.2	98.7
21	90.4	3.33	0.14	0.14	1.50	6.13	101.6
22	85.1	9.00	0.49	0.03	2.79	4.29	101.7
23	66.7	30.6	0.07	0.32	0.49	2.33	100.6
24	82.1	5.51	0.67	0.05	3.36	9.51	101.2
25	24.4	71.2	0.08	0.22	3.14	0.86	99.9
26	73.7	22.0	0.80	0.09	1.72	3.23	101.5
27	43.9	56.4	0.01	0.02	0.96	0.13	101.4
28	47.2	52.5	0.06	0.01	0.58	0.05	100.4

LOI: loss of ignition.

by XRD analysis, compared to XRF data. As XRD-Rietveld results are normalized to 100 wt %, deviations in a single phase affect proportions of all other phase in the mixture.

## CONCLUSION

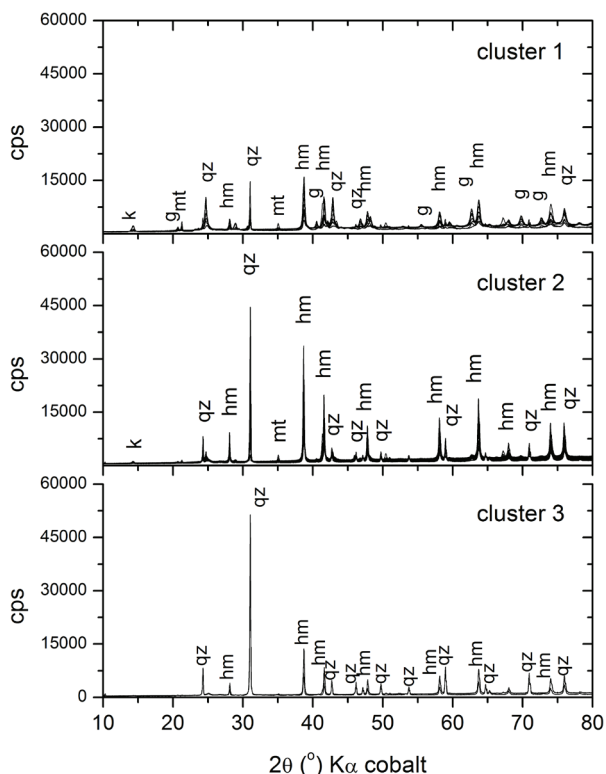
Iron ore is usually classified in terms of its total iron content. However, chemical data does not indicate the proportion of mineral phases in the ore, which is a relevant parameter to be considered in ore treatment, seeing aspects such as grindability, fuel consumption and CO<sub>2</sub> emission.

A low-cost and reliable alternative to chemical classification combines XRD-Rietveld quantitative phase analysis and cluster analysis. Detailed analyses of a representative set of samples by XRD-Rietveld and XRF allow definition of the main types of

**Table 2.** Mineralogical composition (wt %) determined by XRD-Rietveld.

Cluster	Sample	hm	mt	go	qz	k	gibb	R <sub>wp</sub>
1	4	52.4	-	39.5	7.4	-	-	10.8
1	5	6.5	-	61.7	19.3	12.6	-	10.0
1	7	12.5	-	55.4	5.5	24.4	2.5	11.5
1*	8	24.1	-	69.8	3.7	0.9	1.4	10.6
1	9	54.4	12.9	27.8	5.6	-	-	11.7
1	20	35.6	-	25.3	3.9	25.2	10.0	10.0
1	21	35.2	2.1	55.1	3.7	-	-	10.0
1	24	17.4	-	71.9	1.9	6.6	2.2	11.5
2	1	38.5	-	8.3	53.3	-	-	14.6
2	2	45.9	0.7	4.6	45.4	3.5	-	13.8
2*	3	46.2	1.8	8.5	41.2	2.4	-	13.6
2	6	38.2	14.3	16.2	31.1	-	-	10.6
2	10	27.0	1.3	19.8	47.3	4.6	-	11.4
2	11	54.2	0.7	13.0	32.1	-	-	12.7
2	12	23.9	1.5	11.0	56.6	7.1	-	14.2
2	13	30.3	1.7	6.4	58.2	3.4	-	13.2
2	14	46.1	1.0	21.7	18.2	13.0	-	10.5
2	15	34.6	5.2	16.1	44.1	-	-	12.1
2	16	80.8	1.0	12.1	1.9	4.1	-	12.0
2	17	22.2	4.8	14.8	47.9	10.3	-	12.5
2	18	64.8	1.2	8.2	21.2	4.6	-	12.3
2	19	80.7	2.0	10.2	7.2	-	-	12.0
2	22	67.0	0.5	20.1	8.9	3.5	-	11.2
2	23	30.7	8.2	21.9	39.2	-	-	11.6
2	26	50.1	0.3	16.0	27.1	6.4	-	11.9
3	25	16.5	-	4.7	73.6	5.1	-	18.2
3*	27	33.0	1.1	4.1	59.9	1.8	-	15.8
3	28	31.6	1.6	5.1	61.7	-	-	16.0

\*Representative sample of each cluster. Hm: hematite; mt: magnetite; go: goethite; qz: quartz; k: kaolinite; gibb: gibbsite; R<sub>wp</sub>: weighted statistical residue of Rietveld refinement.



K: kaolinite; g: goethite; mt: magnetite; hm: hematite; qz: quartz; CPS: counts per second.

**Figure 3.** Diffractograms of iron ore samples, divided in cluster 1, cluster 2 and cluster 3.

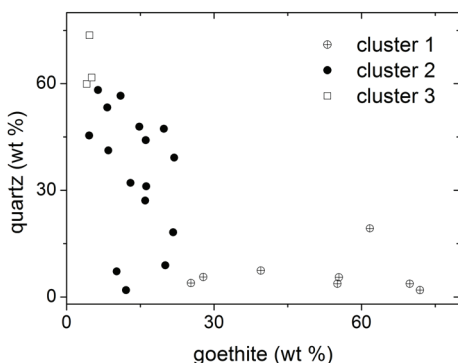


**Figure 4.** Goethite and quartz abundance (wt %) of the three clusters. Phase proportions were determined by XRD-Rietveld.

ore, which are defined as clusters. After defining representative clusters for a given deposit, samples are sorted directly from their raw XRD patterns, with no need to analyze individual data.

Whole-rock chemical data is an important reference for cross-checking results of mineralogical analysis. Comparison between XRD and XRF data is an important step in the

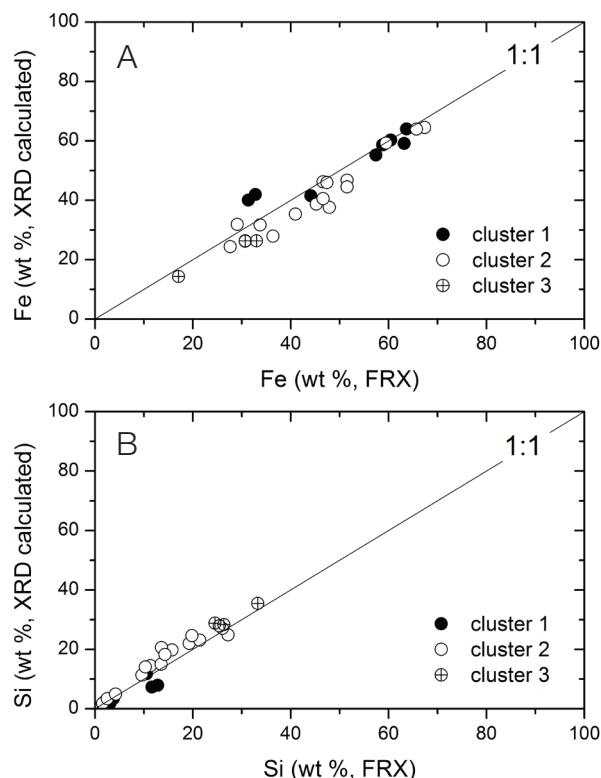


**Figure 5.** Comparison between chemical and mineralogical data. (A) Fe: XRF vs. XRD,  $R^2 = 0.9034$ ; (B) Si: XRF vs XRD,  $R^2 = 0.9406$ .

development of Rietveld refinement strategies. XRD-Rietveld refinement results show good agreement with whole-rock chemical data. Additionally, hematitic iron ores are suitable materials for quantitative XRD analysis, since the main phases (hematite, magnetite, goethite, quartz, kaolinite) show little overlapping of diffraction peaks.

The studied set of iron ore samples was divided into three clusters: cluster 1, with amounts of hydrated phases, indicating the influence of weathering processes; cluster 2, which represents samples of primary hematitic ore, composed mainly by hematite and quartz; and cluster 3, that represents low-grade ores, in which quartz largely predominates over hematite. Magnetite is not an essential phase in this type of ore, with erratic distribution and contents  $< 2$  wt % in most samples. Iron ores classification by XRD-Rietveld and cluster analysis is a fast, low-cost and reliable option for chemical analysis.

## ACKNOWLEDGEMENTS

The authors would like to thank engineer Guilherme Soares and Usiminas S. A., for providing samples and chemical data, as well as the comments of two anonymous reviewers.

## REFERENCES

- Antoniassi, J. L., Tassinari, M. M. M. L., Kahn, H., Gobbo, L. (2008). Análise grupal por difratometria de raios X em apoio à exploração e geometalurgia. *XLIV Congresso Brasileiro de Geologia*, 208. Curitiba: SBG.
- Babinski, M., Chemale Júnior, F., van Schmus, W. R. (1993). A idade das formações ferríferas bandadas do Supergrupo Minas e sua correlação com aquelas da África do Sul e da Austrália. *II Simpósio do Cráton do São Francisco*, 152-153. Salvador: SBG.
- Bish, D. L., von Dreele, R. B. (1989). Rietveld refinement of non-hydrogen atomic positions in kaolinite. *Clays and Clay Minerals*, 37(4), 289-296.
- Caglioti, G., Paoletti, A., Ricci, F. P. (1958). Choice of collimators for a crystal spectrometer for neutron diffraction. *Nuclear Instruments*, 3(4), 223-228.
- Chemale Júnior, F., Rosière, C. A., Endo, I. (1994). The tectonic evolution of the Quadrilátero Ferrífero, Minas Gerais, Brazil. *Precambrian Research*, 65(1-4), 25-54.
- Departamento Nacional de Produção Mineral (2013). *Sumário mineral*. Brasília: DNPM. Acesso em: 20 de novembro de 2014, <<https://sistemas.dnmp.gov.br/>>.
- Departamento Nacional de Produção Mineral (2014). *Informe mineral 1.º/2014*. Brasília: DNPM. Acesso em: 20 de novembro de 2014, <[http://www.dnmp.gov.br/mostra\\_arquivo.asp?IDBancoArquivoArquivo=9328](http://www.dnmp.gov.br/mostra_arquivo.asp?IDBancoArquivoArquivo=9328)>.
- Dorr, J. V. N. (1969). *Physiographic, stratigraphic and structural development of the Quadrilátero Ferrífero, Minas Gerais*. Professional Paper 641-A. EUA: United States Geological Survey.
- Everitt, B. S., Landau, S., Leese, M., Stahl, D. (2011). *Cluster analysis*. Nova York: Wiley.
- Grazulis, S., Chateigner, D., Downs, R. T., Yokochi, A. T., Quirós, M., Lutterotti, L., Manakova, E., Butkus, J., Moeck, P., LeBail, A. (2009). Crystallography open database: an open-access collection of crystal structures. *Journal of Applied Crystallography*, 42(Pt 4), 726-729.
- Ikuta, D., Kawame, N., Banno, S., Hirajima, T., Ito, K., Rakovan, J. F., Downs, R. T., Tamada, O. (2007). First in situ X-ray identification of coesite and retrograde quartz on a glass thin section of an ultrahigh-pressure metamorphic rock and their crystal structure details. *American Mineralogist*, 92(1), 57-63.
- Knorr, K., Yang, N. (2011). Quantitative X-ray mineralogy of iron ore and scales. *Iron Ore Conference*, 265-269. Perth: AusIMM.
- Levy, D., Giustetto, R., Hoser, A. (2012). Structure of magnetite (Fe<sub>3</sub>O<sub>4</sub>) above the Curie temperature: a cation ordering study. *Physics and Chemistry of Minerals*, 39(2), 169-176.
- Li, D., O'Connor, H., Low I., van Riessen, A., Toby, B. H. (2006). Mineralogy of Al-substituted goethites. *Powder Diffraction*, 21(4), 289-299.
- McCusker, L. B., von Dreele, R. B., Cox, D. E., Louër, D., Scardi, P. (1999). Rietveld refinement guidelines. *Journal of Applied Crystallography*, 32, 36-50.
- Parian, M., Lamberg, P., Möckel, R., Rosenkranz, J., (2015). Analysis of mineral grades for geometalurgy: combined element-to-mineral conversion and quantitative X-ray diffraction. *Minerals Engineering*, 82, 25-35.
- Pena, Q. E., Rosière, C. A., Seshadri, V. (2003). Avaliação técnica de minérios de ferro para sinterização nas siderúrgicas e minerações brasileiras: uma análise crítica. *Revista Escola de Minas*, 56(2), 97-102.
- Renger, F. E., Noce, C. M., Romano, A. W., Machado, N. (1995). Evolução sedimentar do Supergrupo Minas: 500 Ma de registro geológico no Quadrilátero Ferrífero, Minas Gerais, Brasil. *Geonomos*, 2(1), 1-11.
- Rietveld, H. M. (1969). A profile refinement method for nuclear and magnetic structures. *Journal of Applied Crystallography*, 2, 65-71.
- Rosière, C. A., Chemale Júnior, F. (2001). Itabiritos e minérios de ferro de alto teor do Quadrilátero Ferrífero: uma visão geral e discussão. *Geonomos*, 8(2), 27-43.
- Saalfeld, H., Wedde, M. (1974). Refinement of the crystal structure of gibbsite, Al(OH)<sub>3</sub>. *Zeitschrift für Kristallographie*, 139, 129-135.
- Sawada, H. (1996). An electron density residual study of  $\alpha$ -ferric oxide. *Materials Research Bulletin*, 31(2), 141-146.
- Shimizu, V. K., Kahn, H., Antoniassi, J. L., Ulsen, C. (2012). Copper ore type definition from Sossego Mine using X-ray diffraction and cluster analysis technique. *Revista Escola de Minas*, 65(4), 561-566.
- Toby, B. H. (2006). R factors in Rietveld analysis: how good is good enough? *Powder Diffraction*, 21(1), 67-70.